MAUN Fen Bil. Dergi., 11:2 55-64, 2023 Araştırma Makalesi/ Research Article
MAUN J. of Sci., 11:2 55-64, 2023 DOIhttps://doi.org/10.18586/msufbd.1353252

Investigation of TEC Changes on Magnetic Conjugate Pairs over the Africa Region during the Geomagnetic Storm of August 25-26, 2018.

Serhat KORLAELCİ[1]
[1]Department of Medical Services and Tecniques, Vocational School of Health Services, Mus Alparslan University, Mus, Turkey

✉: s.korlaelci@alparslan.edu.tr [1]0000-0002-0956-4721

Received (Geliş): 31.08.2023 Revision (Düzeltme): 20.11.2023 Accepted (Kabul): 05.122023

ABSTRACT

In this study, we investigated two magnetic conjugate pairs over the African region during the geomagnetic storm of August 25-26, 2018. The effects of geomagnetic conditions, represented by the Dst index and IMF Bz values, on the Total Electron Content (TEC) values at the conjugate stations were compared for stormy and quiet periods. During the storm period, the effect of the TEC values at the stations in the northern hemisphere on the TEC values at the stations in the southern hemisphere is greater than the effect of the TEC values in the southern hemisphere on the TEC values in the northern hemisphere. According to this result, it can be said that the southward electromagnetic convection was more than the northward convection during the dates examined. When the coefficients are analyzed, it can be said that the interaction is higher in the magnetic conjugate pair closer to the equator during the storm period, while the interaction is higher in the magnetic conjugate pair farther from the equator during the quiet period. When the coefficients calculated for Dst and IMF Bz are considered, it is seen that the TEC values are very small compared to their coefficients. It can be concluded that the effect of Dst and IMF Bz is much smaller than the effect of TEC values at a station on TEC values at its magnetic conjugates.

Keywords: Ionosphere, Autoregressive Distributed Lag, magnetic conjugate pairs, Total Electron Content, geomagnetic storm

25-26 Ağustos 2018 Jeomanyetik Fırtına Sırasında Afrika Bölgesi Üzerindeki Manyetik Eşlenik Çiftleri Üzerindeki TEC Değişikliklerinin İncelenmesi

ÖZ

Bu çalışmada, 25-26 Ağustos 2018 jeomanyetik fırtınası sırasında, Afrika bölgesi üzerinde iki manyetik eşlenik çifti incelendi. Dst indeksi ve IMF Bz değerleri ile sunulan jeomanyetik koşulların, eşlenik istasyonlardaki Toplam Elektron İçeriği (TEC) değerleri üzerindeki etkileri fırtınalı ve sessiz dönemler için karşılaştırılmıştır. Fırtına döneminde kuzey yarımküredeki istasyonlardaki TEC değerlerinin güney yarımküredeki istasyonlardaki TEC değerlerine etkisi, güney yarımküredeki TEC değerlerinin kuzey yarımküredeki TEC değerlerine etkisinden daha fazladır. Bu sonuca göre incelenen tarihlerde güney yönlü elektromanyetik taşınımın kuzey yönlü taşınımdan daha fazla olduğu söylenebilir. Katsayılar incelendiğinde fırtına döneminde ekvatora daha yakın olan manyetik eşlenik çiftinde etkileşimin daha fazla olduğu, sessiz dönemde ise ekvatora uzak olan manyetik eşlenik çiftinde etkileşimin daha fazla olduğu söylenebilir. Dst ve IMF Bz için hesaplanan katsayılar dikkate alındığında TEC değerlerinin katsayılarına göre çok küçük olduğu görülmektedir. Buradan Dst ve IMF Bz'nin etkisinin, bir istasyondaki TEC değerlerinin, manyetik eşleniklerindeki TEC değerleri üzerindeki etkisinden çok daha küçük olduğu sonucuna varılabilir.

Anahtar Kelimeler: İyonosfer, Otoregresif Dağıtılmış Gecikme, Manyetik Eşlenik noktalar, Toplam Elektron İçeriği, Jeomanyetik Fırtına

INTRODUCTION

Ninety percentage of intense geomagnetic storms (Dst ≤-100 nT) are caused by the effect of Coronal Mass Ejections (CME) [1, 2]. The major source of strong space weather irregularities occurring on Earth is considered to be CME [3, 4]. The slow-moving CME that occurred on August 20, 2018, appeared to have turned into a large geomagnetic storm, although it was expected to cause a minor storm. The August 26, 2018 space weather event is known as the largest storm at the minimum phase of 24th solar cycle, after two major geomagnetic storms in 2015 [5]. This storm has been studied with different aspects in many studies [6–8]. Storms are closely related to physical processes in the ionosphere [9].

The effects of geomagnetic storms on the ionosphere can significantly change parameters such as electron density and Total Electron Content (TEC) [10]. During the storm,

vertical plasma drift occurs in the equatorial ionosphere due to changes in the electric field. When the field is eastward it causes strong plasma drift. When the electrical field is westward it causes weak plasma drift. That is, eastward plasma drift increases the irregularities, while westward drift decreases it [11, 12]. The proof of the formation of ionospheric irregularities is also expressed as rapid decrease in TEC values [13]. TEC is the number of electrons in a cylinder of unit cross section along the signal path between a satellite and its receiver. The unit of TEC is TECU and 1 TECU is 10^{16} electrons/m^2 [14].

The special electrodynamic processes such as the equatorial ionization anomaly (EIA), the Post Sunset Rise (PSSR), the Rayleigh−Taylor instability (RTI), and Equatorial Plasma Bubbles (EPBs) is effected to equatorial ionosphere [15, 16]. These electrodynamic processes cause increased ionization in the equatorial region (about ± 15 degrees of the magnetic equator)[12, 17]. Another process that affects the ionization process is the connection between the ionospheric magnetic conjugate points formed by the high electrical conductivity in the geomagnetic field. This connection causes ionospheric changes at the conjugate points [18].

In the magnetosphere-ionosphere system, intense electric fields and currents are always excited and their effects are global. These effects, which are also caused by geomagnetic storms, occur simultaneously in the polar regions and spread to the equator [19]. Hanson (1963) first proposed the possibility of photoelectron transfer between magnetic conjugate points. Unlike charged thermal energy particles, photoelectrons can establish a direct link between their magnetic conjugate regions [20]. Since then the relationship between magnetic conjugate points has been studied by many researchers [21–28].

Significant progress has been made in identifying sources of irregularities in TEC, such as coronal mass ejection, galactic and cosmic rays, earthquakes, volcanoes, typhoons [29–32]. However, there is still a need to increase the measurement accuracy rate even further. In this context, the interaction of TEC measurements obtained between magnetic conjugate points should be considered. In this study, the relationship between TEC measurements obtained from two pairs of magnetic conjugate GPS (Global Positioning System) stations in the African low latitude region was examined for the August 26, 2018, geomagnetic storm and calm conditions. In addition, the interaction rates obtained in this study were compared with the Dst index, which is the main indicator of the changes in the geomagnetic field in the equatorial region, and the effect of the z-direction component of the interplanetary magnetic field (IMF Bz).

MATERIAL and METHOD

In the present study, two magnetic conjugate pairs were identified to investigate the ionospheric TEC changes in the African region. These pairs are Haifa (32.77º N, 35.02º E)- Ambalavao (21.90º S,46.79º E) and Djibouti (11.52º N, 42.84º E)-Malindi (2.99º S, 40.19º E) and their geographic locations are shown in Figure 1. Their geographic and geomagnetic coordinates are given in Table 1 and were obtained from the World Data Center for Geomagnetism (http://wdc.kugi.kyoto-u.ac.jp/igrf/gggm/).The GPS receiver data for these stations are obtained from (https://network.igs.org/) of the IGS for the period of 1-7 August 2018 and 25-31 August 2018, in Receiver INdependent EXchange (RINEX) format. These data were converted to 30-second VTEC data by the IONOLAB-TEC/STEC software on the Ionospheric Research Laboratory (IONOLAB) (http://www.ionolab.org/) [33–35].

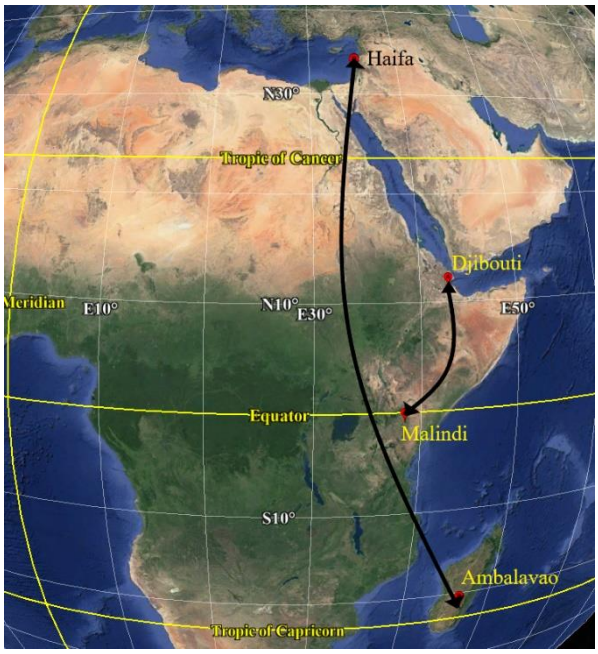

Figure 1: Geographic coordinates of two different magnetic conjugate pairs over the African region.

Table 1: Geographic and geomagnetic coordinates of the stations where TEC data was obtained.

Station Name	Geographic Coordinates		Geomagnetic Coordinates	
	Latitude	Longitude	Latitude	Longitude
Haifa	32.77º N	35.02º E	29.78º N	113.16º E
Ambalavao	21.90º S	46.79º E	26.84º S	116.06º E
Djibouti	11.52º N	42.84º E	7.49º N	117.50º E
Malindi	2.99º S	40.19º E	7.28º S	112.13º E

The time for the geomagnetic storm period, the date range from 25-31 August 2018 was chosen. To determine the geomagnetic storm period, Dst, Kp values which are the indicators of the changes in the geomagnetic field, and IMF Bz values, which is the z component of the interplanetary magnetic field, were obtained from the NASA Space Physics Data Facility (SPDF)(https://omniweb.gsfc.nasa.gov/form/dx1.html).

The main phase of the storm (26 August 2018) was determined by considering the maximum changes in these indices. The storm period was determined as the date range (25-31 August 2018) covering three days before and after the main phase. The time frame for the quiet period, the date range from 1-7 August 2018 was chosen. The temporal changes in IMF Bz and geomagnetic indices for these periods are given in Figure 2.

The positive values of Dst, which indicates the initial phase of the geomagnetic storm, started at 03:00 UT on August 25 and continued until 17:00 UT. During this time, the IMF Bz value changed from 0.4 nT to -6.3 nT, and the Kp value changed from 1.0 to 1.7. Then, the main phase of the storm, which started at about 18:00 on August 25, ended at 06:00 UT on August 26. During the main phase, the Dst value reached a maximum of -175 nT. During this period, the IMF Bz value changed from -8.9 nT to -12.7 nT, and the Kp value changed from 3.7 to 7.3. It is seen that the storm's return phase started from approximately 06:00 UT on August 26. All these results represent a geomagnetic storm process [36, 37]. Dst value varies between -10 and 19 nT, and Kp value varies between 0 and 3 in the date range of 1-7 August 2018, which we have determined as the quiet period. Considering, Kp < 3; the Dst < -50 nT values for quiet period as a reference, it is compatible with the literature [38, 39].

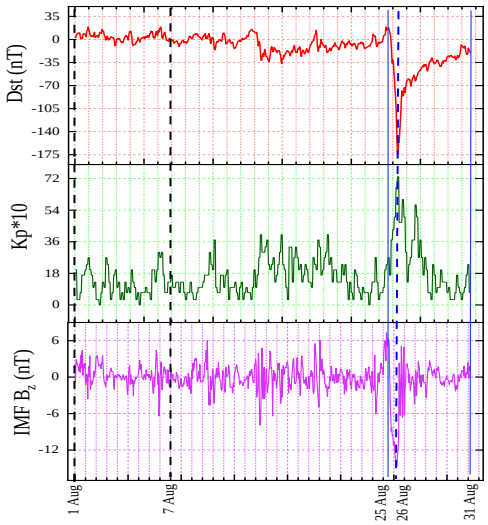

Figure 2: Temporal changes of IMF Bz, Kp index, and Dst indices during 1-31 August 2018. The black dashed vertical lines in the figure represent the quiet period range. The blue vertical dashed line represents the maximum storm time and the blue vertical lines the storm period.

The Autoregressive Distributed Lag (ARDL) approach developed by Pesaran et al. (2001) was used to examine the relationship between the variables [40]. When the variables are integrated of different order (I (0) or I (1)), the cointegration relationship between the variables can be analyzed with the ARDL method (See, for example,). Therefore, the ARDL estimation technique is one of the most appropriate when the integration order of the variables is different. Moreover, according to Pesaran and Shin (1999), the ARDL technique produces consistent results in the case of autocorrelation and endogeneity problems [40, 41].

$$\Delta Y_t = \gamma_0 + \sum_{i=1}^{n} \gamma_i \Delta Y_{t-i} + \sum_{i=1}^{n} \delta_i \Delta X_{t-i} + \varphi_1 Y_{t-1} + \varphi_2 X_{t-1} + \varepsilon_t \quad (1)$$

Y_t and X_t are the dependent and independet variables, respectively. γ_0, γ_i, δ_i, φ_1, φ_2 are the coefficient of the variables. The significance of the lagged variables in Eq. (1) is determined by the F test. However, the asymptotic distribution of the F-statistics is non-standard. Therefore, the critical values produced by Pesaran et al. (2001) are used. The cointegration relationship between the variables in Eq. (1) is determined by testing $\alpha_1 = \alpha_2 = 0$ hypotheses. Following the estimation of Eq. (1) with the ARDL method, the joint significance of the α_1 and α_2 coefficients are tested using the F test statistic. The variables are cointegrated if the calculated F statistic is greater than the critical upper bound. If the F value is less than the critical lower bound, it means that there is no cointegration among the underlying variables. If the calculated F statistics fall between the lower and upper bounds, it is inconclusive. Hence, no decision can be made by using the bound test.

The ARDL model, which is a powerful statistical model, was applied to reveal how much any magnetic conjugate point is affected by the other magnetic conjugate point and by the geomagnetic index (Dst) and IMF B_z. The ARDL model is a linear time series model in which both dependent and independent variables have a relationship, in which the lagged and level values are integrated.
Time series must be stationary to be analyzed statistically. The unit root test determines whether the series in a data set are stationary. If the series are stationary, that is, it has no unit root, it has a finite variance. In this study, stationarity analysis was performed by two different unit root tests (Augmented Dickey-Fuller (ADF) and Phillips-Perron (PP)), which are widely used [42–44]. The equation has been formulated as follows.

$$\Delta Y_t = \mu + \beta_t + \delta Y_{t-1} + \sum_{j=1}^{k} \alpha_j \Delta Y_{t-j} + \varepsilon_t \quad (2)$$

where Y_t is the variable under stationary test, Δ is the difference operator, μ, β, δ and α are the equation coefficients, t is a time trend, ε_t is the error term, and k is the optimal lag length.

RESULTS and DISCUSSION

The interaction rates of TEC values at conjugate stations and the interaction rates from solar and geomagnetic indices for two magnetic conjugate pairs selected over

the African region were examined by the statistical ARDL model in this study. In this model, the stationarity of dependent and independent variables was analyzed first. The unit root test results of the dependent variable (TEC) and independent variables (Dst and IMF Bz) data in the analyses are given in Table 2. If the absolute value of the coefficients of the variables given in this table is greater than the MacKinnon (1996) critical values in Table 2 and the probability value in the parentheses is significant, it is stationary according to the unit root test [45]. For example, the ADF unit root coefficient in Haifa TEC's Quiet Days is -5.50 and its probability value is (0.0000). The absolute value of this number is higher than the MacKinnon (1996) critical values (-4.09, -3.47, -3.16) and the probability value is less than 0.01. In this case, it is stated that the Haifa TEC values are stationary at 1% (this ratio is expressed with an * sign). If the probability value is not significant at the level, the first difference is checked and if it is not significant, it is concluded that the data set is not suitable for analysis. According to the results in the table, it is seen that the variables in the data set were stationary at the level or the first difference.

Table 2: Unit Root Test results

	Variables	Quiet Days		Storm Days	
		ADF	**PP**	**ADF**	**PP**
Level	**Haifa TEC**	-5.50	-3.88	-4.94	-3.19
	(Probability)	(0.0000)*	(0.0028)*	(0.0001)*	(0.0230)*
	Ambalavao TEC	-7.28	-3.61	-3.93	-3.01
	(Probability)	(0.0000)*	(0.0066)*	(0.0024)*	(0.0365)*
	Djibouti TEC	-8.46	-3.94	-8.46	-3.80
	(Probability)	(0.0000)*	(0.0123)**	(0.0000)*	(0.0035)*
	Malindi TEC	-6.13	-3.82	-6.77	-3.80
	(Probability)	(0.0000)*	(0.0176)**	(0.0000)*	(0.0035)*
	Dst	-4.14	-3.16	-2.30	-2.15
	(Probability)	(0.0011)*	(0.0242)**	(0.1727)	(0.2243)
	IMF B_z	-5.21	-5.23	-3.08	-3.69
	(Probability)	(0.0000)*	(0.0000)*	(0.0298)**	(0.0051)
First Difference	**Haifa TEC**	-5.99	-6.49	-3.68	-7.03
	(Probability)	(0.0000)*	(0.0000)*	(0.0055)*	(0.0000)*
	Ambalavao TEC	-5.02	-6.57	-5.72	-5.47
	(Probability)	(0.0000)*	(0.0000)*	(0.0000)*	(0.0000)*
	Djibouti TEC	-8.73	-7.45	-9.03	-8.16
	(Probability)	(0.0000)*	(0.0000)*	(0.0000)*	(0.0000)*
	Malindi TEC	-5.73	-5.76	-6.22	-6.30
	(Probability)	(0.0000)*	(0.0000)*	(0.0000)*	(0.0000)*
	Dst	-9.82	-10.71	-6.73	-6.74
	(Probability)	(0.0000)*	(0.0000)*	(0.0000)*	(0.0000)*
	IMF B_z	-14.41	-23.65	-5.96	-13.41
	(Probability)	(0.0000)*	(0.0000)*	(0.0000)*	(0.0000)*

MacKinnon (1996) critical values	**ADF**	**PP**	**The level of significance**
	-4.09	-4.08	1%
	-3.47	-3.47	5%
	-3.16	-3.16	10%

(*), (**), (***) indicate 1%, 5% and 10% significance levels, respectively. Considered according to MacKinnon (1996).

Transports between magnetic conjugate points occur through electromagnetic processes [19]. This movement may be from the Northern Hemisphere to the Southern Hemisphere, or it may be in the opposite direction. For this reason, the TEC value at each station was evaluated separately as the dependent variable to see the effect of bidirectional transport in magnetic conjugate pairs.

Haifa-Ambalavao Magnetic Conjugate Pair

The regression analysis equation, which is also used in many ionospheric studies, was used to examine the TEC changes of the Haifa - Ambalavao magnetic conjugate pair during the storm period (25-31 Aug 2018) [46, 50]. This equation returns the result of the relationship between the variables as a coefficient. Accordingly, the regression equations for the two stations during the storm period are given as follows.

$$(\mathrm{TEC_{Haifa}}) = \alpha_0 + \alpha_1(\mathrm{TEC_{Ambalavao}}) + \alpha_2(\mathrm{Dst}) + \alpha_3(\mathrm{IMF\ B_z}) + \varepsilon \quad (3)$$

$$(\mathrm{TEC}_{\mathrm{Ambalavao}}) = \beta_0 + \beta_1(\mathrm{TEC}_{\mathrm{Haifa}}) + \beta_2(\mathrm{Dst}) + \beta_3(\mathrm{IMF\ B_z}) + \varepsilon \quad (4)$$

For the quiet period on 1-7 Aug 2018, the interaction of the magnetic conjugate points with each other was examined. The equations for the quiet period are as follows.

$$(\mathrm{TEC}_{\mathrm{Haifa}}) = \alpha_0 + \alpha_1(\mathrm{TEC}_{\mathrm{Ambalavao}}) + \alpha_2(\mathrm{Dst}) + \alpha_3(\mathrm{IMF\ B_z}) + \varepsilon \quad (5)$$

$$(\mathrm{TEC}_{\mathrm{Ambalavao}}) = \beta_0 + \beta_1(\mathrm{TEC}_{\mathrm{Haifa}}) + \beta_2(\mathrm{Dst}) + \beta_3(\mathrm{IMF\ B_z}) + \varepsilon \quad (6)$$

where (α_0, β_0) denotes the regression constant $\alpha_1, \alpha_2, \alpha_3, \beta_1, \beta_2, \text{and } \beta_3$, regression coefficients and ε the error term. The existence of the relationship between the dependent and independent variables was examined by the ARDL bounds test approach. The validity of the test for the model under consideration was made by calculating the F-statistics and by comparing the Pesaran et al. (2001) critical values. The F-statistics values obtained for equations (3), (4), (5), and (6) were found to be at a significance level of 1% according to the Pesaran et al. (2001) critical values. In this situation, it is understood that the F statistical values given in the Table 3 are greater than the Pesaran et al. (2001) critical values. This result shows that the statistical expressions established by equations (3), (4), (5) and (6) are meaningful.

Table 3: ARDL F-Bounds Test Results of Haifa-Ambalavao magnetic pair

	Equation 3	Equation 4	Equation 5	Equation 6
F-statistic	(7.70)*	(7.86)*	(8.77)*	(16.82)*

Pesaran et al. (2001) critical values		
Signif.	**I(0)**	**I(1)**
10%	3.03	4.06
5%	3.47	4.57
2.5%	3.89	5.07
1%	4.4	5.72

Critical values were taken from Pesaran et al. (2001), from Table CI (iii). (*) indicates 1% significance level.

Assumption tests were performed to examine the fit of the model. Diagnostic tests are essential for consistent results. For example, the relationship between the error terms reveals the existence of autocorrelation. In the case ofautocorrelation, least squares estimators of parameters are unbiased and consistent, but ineffective. Similarly, in the case of heteroscedasticity, the minimum variance property of the parameters is no longer valid. If heteroscedasticity exists, the estimation efficiency decreases. As a rule of thumb, if the probability value of the diagnostic tests is greater than 0.05, which is a commonly used confidence level in statistics, the desired properties are valid. The results of the various diagnostic tests are shown in Table 4. The coefficient of the diagnostics test varies depending on the number of observations, the number of explanatory variables, and the significance level. First, the Ramsey-Reset test confirms that the functional form used for the estimations is accurate. Second, the result of the Breusch-Godfrey LM test shows that serial correlation is not present in our estimations. Third, the result of the Jarque-Berra test statistic shows that the residuals are normally distributed. Fourth, Breusch-Pagan-Godfrey test results validate those residuals are homoscedastic. Last, CUSUM and CUSUMQ (Cumulative sum and cumulative sum of squares) tests confirm the stability property of the models.

Table 4: Hypothesis tests of the Haifa – Ambalavao magnetic conjugate pair.

	Equation 3		Equation 4		Equation 5		Equation 6	
	F-Statistic	**(prob.)**	**F-Statistic**	**(prob.)**	**F-Statistic**	**(prob.)**	**F-Statistic**	**(prob.)**
Breusch-Godfrey LM Test	0.44	0.64	0.42	0.66	1.32	0.27	1.84	0.16
Jarque-Bera Test	3.67	0.15	1.31	0.51	0.48	0.78	0.11	0.94
Breusch-Pagan-Godfrey	0.54	0.92	1.04	0.41	0.85	0.69	1.25	0.20
Ramsey	0.42	0.67	1.99	0.16	0.01	0.91	2.85	0.09
Cusum	stable	stable	stable	stable	stable	stable	stable	stable
Cusumq	stable	stable	stable	stable	stable	stable	stable	stable

According to these test results, the ARDL model to be applied to the equations was found to be appropriate. The results of the ARDL model are given in Table 5. When the coefficient values for Eq. (3) are investigated, a change of 1% in the TEC value at the Ambalavao station causes an increase of 0.414% in the TEC value at the Haifa station, which is the magnetic conjugate point. A 1 nT change in Dst and IMF Bz causes a decrease of 0.003 TECU / an increase of 0.028 TECU in the TEC value at the Haifa station, respectively. In addition, the coefficient of error correction term of -0.25 indicates that the effect of TEC change at Haifa station will stabilize at a rate of 25% every hour starting from the first hour.

When the coefficient values for Eq. (4) were investigated, a change of 1% in the TEC value at the Haifa station causes an increase of 0.611% in the TEC value at the Ambalavao station, which is the magnetic conjugate point. A change of 1 nT in the Dst and IMF Bz index causes a decrease of 0.015 TECU / an increase of 0.036 TECU in TEC at Ambalavao station, respectively. In addition, the coefficient of error correction term of -0.37 indicates that the effect of TEC change at Ambalavao station will stabilize at a rate of 37% every hour starting from the first hour.

When the coefficient values for Eq. (5) were investigated, a change of 1 % in the TEC value at Ambalavao station causes a decrease of 2.85% in the TEC value at Haifa station, which is the magnetic conjugate point. A change of 1 nT in the Dst index causes a decrease of 0.006 TECU in the TEC value at the Haifa station. Since the probability value (>0.05) in IMF Bz is insignificant, no statistical result can be said for this coefficient. The coefficient of error correction term of -0.29 shows that the effect of TEC change in Haifa station will stabilize at a rate of 29% every hour starting from the first hour.

When we look at the coefficient values for Eq. (6), a change of 1% in the TEC value at the Haifa station causes an increase of 10.05% in the TEC value at the Ambalavao station, which is the magnetic conjugate point. Since the probability value (>0.05) in the Dst index and IMF Bz is insignificant, an evaluation cannot be made for these coefficients. In addition, the coefficient of error correction term of -0.30 shows that the effect of TEC change at Ambalavao station will stabilize at a rate of 30% every hour starting from the first hour.

Table 5: Equation coefficients in ARDL model of Haifa – Ambalavao magnetic conjugate pair.

	Equation 3			**Equation 4**	
Variable	**Coefficient**	**Prob.**	**Variable**	**Coefficient**	**Prob.**
Ambalavao TEC	0.414	(0.000)*	**Haifa TEC**	0.411	(0.000)*
Dst	-0.003	(0.058)***	**Dst**	-0.015	(0.023)**
IMF B_z	0.028	(0.061)***	**IMF B_z**	0.036	(0.052)***
CointEq(-1)	-0.25	(0.000)*	**CointEq(-1)**	-0.37	(0.000)*
	Equation 5			**Equation 6**	
	Coefficient	**Prob.**		**Coefficient**	**Prob.**
Ambalavao TEC	-2.85	(0.004)*	**Haifa TEC**	10.05	(0.001)*
Dst	-0.006	(0.036)**	**Dst**	0.002	(0.66)
IMF B_z	- 0.010	(0.39)	**IMF B_z**	-0.018	(0.35)
CointEq(-1)	-0.29	(0.000)*	**CointEq(-1)**	-0.30	(0.000)*

Critical values were taken from Pesaran et al. (2001), from Table CI (iii). (*) indicates 1% significance level.

Djibouti-Malindi Magnetic Conjugate Pair

The regression equations established to examine the TEC changes of the Djibouti-Malindi magnetic conjugate pair during the storm period (25-31 Aug 2018) are given below:

$$(\mathrm{TEC_{Djibouti}}) = \alpha_0 + \alpha_1(\mathrm{TEC_{Malindi}}) + \alpha_2(\mathrm{Dst}) + \alpha_3(\mathrm{IMF\ B_z}) + \varepsilon \quad (7)$$

$$(\mathrm{TEC_{Malindi}}) = \beta_0 + \beta_1(\mathrm{TEC_{Djibouti}}) + \beta_2(\mathrm{Dst}) + \beta_3(\mathrm{IMF\ B_z}) + \varepsilon \quad (8)$$

$$(\mathrm{TEC_{Djibouti}}) = \alpha_0 + \alpha_1(\mathrm{TEC_{Malindi}}) + \alpha_2(\mathrm{Dst}) + \alpha_3(\mathrm{IMF\ B_z}) + \varepsilon \quad (9)$$

$$(\mathrm{TEC_{Malindi}}) = \beta_0 + \beta_1(\mathrm{TEC_{Djibouti}}) + \beta_2(\mathrm{Dst}) + \beta_3(\mathrm{IMF\ B_z}) + \varepsilon \quad (10)$$

When the F-statistics values obtained for equations (7), (8), (9), and (10) were compared with the critical values in Table 6, the significance level was found to be at a significance level of 1%. This result shows that there is a relationship between the variables in equations (7), (8), (9), and (10).

The regression equations that indicate the interaction of the same magnetic conjugate points with each other during the calm period on 1-7 Aug 2018 are as follows:

Then, assumption tests were performed to examine the fit of the model. The results of the assumption tests were shown in Table 7. When the results obtained were examined, the accuracy of these test results, like the assumption tests in the previous magnetic conjugate pair, was found to be > 0.05 in the table (prob.). Again, according to the results of the CUSUM and CUSUMQ tests, it was seen that the coefficients were stable, and the model was stable during the estimation period.

Table 6: ARDL F-Bounds Test Results of Dijibuti-Malindi magnetic pair

	Equation 7	Equation 8	Equation 9	Equation 10
F-statistic	(13.48)*	(10.51)*	(11.45)*	(6.64)*
Pesaran vd. (2001) critical values				
Signif.	**I(0)**	**I(1)**		
10%	3.03	4.06		
5%	3.47	4.57		
2.5%	3.89	5.07		
1%	4.4	5.72		

Critical values were taken from Pesaran et al. (2001), from Table CI (iii). (*) indicates 1% significance level.

Table 7: Hypothesis tests of the Djibouti-Malindi magnetic conjugate pair.

	Equation 7		Equation 8		Equation 9		Equation 10	
	F-Statistic	**(prob.)**	**F-Statistic**	**(prob.)**	**F-Statistic**	**(prob.)**	**F-Statistic**	**(prob.)**
Breusch-Godfrey LM Test (SERIAL)	0.58	0.55	0.61	0.54	0.29	0.74	1.93	0.14
Jarque-Bera Test (NORMALITY)	1.94	0.37	5.30	0.07	1.85	0.39	5.66	0.06
Breusch-Pagan-Godfrey	1.57	0.07	1.17	0.09	0.58	0.86	1.13	0.34
Ramsey	0.15	0.87	0.86	0.38	0.14	0.70	0.63	0.52
Cusum	stable	stable	stable	stable	stable	stable	stable	stable
Cusumq	stable	stable	stable	stable	stable	stable	stable	stable

Table 8 shows the results obtained by the ARDL model for the Djibouti-Malindi magnetic conjugate pair. When the coefficient values for equation (7) are examined, a change of 1% in the TEC value at the Malindi station causes a decrease of 0.57% in the TEC value at the Djibouti station. Since the Dst index and IMF B_z (prob.) were >0.05, it was seen that there was no meaningful relationship. The coefficient of error correction term of -0.59 shows that the effect of TEC change at Djibouti station will stabilize at a rate of 59% per hour starting from the first hour.

When the coefficient values for Eq. (8) are examined, a change of 1% in the TEC value at the Djibouti station causes an increase of 9.69% in the TEC value at the Malindi station. Again, there was no meaningful relationship because the Dst index and IMF B_z (prob.) were >0.05. In addition, the coefficient of error correction term of -0.32 shows that the effect of TEC change at Malindi station will stabilize at a rate of 32% per hour starting from the first hour.

When the coefficient values for Eq. (9) are examined, a change of 1% in TEC value at Malindi station causes a decrease of 1.02% in TEC value at Djibouti station. Since coefficient. The coefficient of error correction term, -0.23, shows that the effect of TEC change at Djibouti station will stabilize at a rate of 23% every hour starting from the first hour. the prob. value in the Dst index and IMF B_z is statistically (>0.05) insignificant, no result can be said for this

Due to the ionospheric conductivity and the effect of neutral winds occurring in the ionosphere, an asymmetric dynamo effect is observed between the conjugate points. Together with the dynamo effect, there is a gradual difference in electrical potentials between the conjugate points. This potential difference is balanced by field-aligned currents occurred between the northern hemisphere and the southern hemisphere [50, 51]. The results obtained for interaction between Djibouti TEC-Malindi TEC, and Ambalavao TEC-Haifa TEC can be explained by the mechanism proposed in Yamazaki (2017).

CONCLUSIONS

The interactions of the TEC changes at two magnetic conjugate pairs in Africa during the storm period (August 25-31, 2018) including the geomagnetic storm on August 26, 2018, and during the quiet period (August 1-7, 2018) were examined and the effect of the geomagnetic Dst and IMF B_z index on these changes were compared.

During the storm period, the effect of TEC values at stations in the northern hemisphere (Haifa and Djibouti) on TEC values at stations in the southern hemisphere (Ambalavao and Malindi) is greater than the effect of TEC values in the southern hemisphere on TEC values in the northern hemisphere. According to this result, it can be said that the south-directed electromagnetic transport is more than the north-directed transport in the examined dates. When the coefficients are examined, it can be said that while the interaction is greater in the magnetic conjugate pair that is closer to the equator in the storm period, it is more in the magnetic conjugate pair that is

Table 8: Equation coefficients of Djibouti-Malindi magnetic conjugate pair in ARDL model.

	Equation 7			Equation 8	
Variable	**Coefficient**	**Prob.**	**Variable**	**Coefficient**	**Prob.**
Malindi TEC	-0.57	(0.000)*	**Djibouti TEC**	9.69	(0.000)*
Dst	0.0001	(0.62)	**Dst**	0.001	(0.404)
IMF B_z	-0.0004	(0.90)	**IMF B_z**	-0.017	(0.172)
CointEq(-1)	-0.59	(0.000)*	**CointEq(-1)**	-0.32	(0.000)*
	Equation 9			**Equation 10**	
	Coefficient	**Prob.**		**Coefficient**	**Prob.**
Malindi TEC	-1.02	(0.037)**	**Djibouti TEC**	0.67	(0.000)*
Dst	-0.007	(0.58)	**Dst**	-0.13	(0.13)
IMF B_z	- 0.002	(0.57)	**IMF B_z**	-0.18	(0.51)
CointEq(-1)	-0.23	(0.000)*	**CointEq(-1)**	-0.19	(0.000)*

(*), (**), (***) indicate 1%, 5% and 10% significance levels, respectively.

far from the equator in the quiet period. Considering the coefficients calculated for Dst and IMF B_z, it is seen that of Dst and IMF B_z is much smaller than the effect of TEC values in a station on the TEC values in its magnetic conjugate.

The obtained results show that the interaction in a magnetic conjugate pair is bidirectional. Therefore, the inclusion of the magnetic conjugate effect in the empirical models is important for the ionospheric delay error estimation.

Acknowledgments

The author would like to thank the IONOLAB group and the International GNSS Service for access to GNSS data to founders for TEC data, used in this study; and the Omni Web Plus NASA/Goddard Space Flight Center service for the data on geomagnetic and solar flux indices.

REFERENCES

[1] Scolini, C., Chané, E., Temmer, M., Kilpua, E.K.J., Dissauer, K., Veronig, A.M., Palmerio, E., Pomoell, J., Dumbović, M., Guo, J., Rodriguez, L. and Poedts, S. CME–CME Interactions as Sources of CME Geoeffectiveness: The Formation of the Complex Ejecta and Intense Geomagnetic Storm in 2017 Early September. The Astrophysical Journal Supplement Series. 247, 1, 21, 2020.

[2] Zhang, J., Richardson, I.G., Webb, D.F., Gopalswamy, N., Huttunen, E., Kasper, J.C., Nitta, N.V., Poomvises, W., Thompson, B.J., Wu, C.-C., Yashiro, S. and Zhukov, A.N. Solar and interplanetary sources of major geomagnetic storms (Dst ≤-100 nT) during 1996–2005. Journal of Geophysical Research: Space Physics. 112, A10, 2007.

[3] Gosling, J.T. Coronal Mass Ejections: An Overview. Geophysical Monograph Series. N. Crooker, J.A. Joselyn, and J. Feynman, eds. American Geophysical Union. 9–16, 2013.

[4] Kilpua, E.K.J., Jian, L.K., Li, Y., Luhmann, J.G. and Russell, C.T. Multipoint ICME encounters: Pre-STEREO and STEREO observations. Journal of Atmospheric and Solar-Terrestrial Physics. 73, 10, 1228–1241, 2011.

[5] Cherniak, I. and Zakharenkova, I. Large-Scale Traveling Ionospheric Disturbances Origin and Propagation: Case Study of the December 2015 Geomagnetic Storm. Space Weather. 16, 9, 1377–1395, 2018.

[6] Blagoveshchensky, D.V. and Sergeeva, M.A. Ionospheric parameters in the European sector during the magnetic storm of August 25–26, 2018. Advances in Space Research. 65, 1, 11–18, 2020.

[7] Yang, Y. -Y., Zhima, Z. -R., Shen, X. -H., Chu, W., Huang, J. -P., Wang, Q., Yan, R., Xu, S., Lu, H. -X. and Liu, D. -P. The First Intense Geomagnetic Storm Event Recorded by the China Seismo-Electromagnetic Satellite. Space Weather. 18, 1, 2020.

[8] Zhang, J., Richardson, I.G., Webb, D.F., Gopalswamy, N., Huttunen, E., Kasper, J.C., Nitta, N.V., Poomvises, W., Thompson, B.J., Wu, C.-C., Yashiro, S. and Zhukov, A.N. Solar and interplanetary sources of major geomagnetic storms (Dst ≤-100 nT) during 1996–2005. Journal of Geophysical Research: Space Physics. 112, A10, 2007.

[9] Richmond, A. D., Lu, G. Upper-atmospheric effects of magnetic storms: a brief tutorial. Journal of Atmospheric and Solar-Terrestrial Physics. 62, 1115–1127, 2000.

[10] Arowolo, O.A., Akala, A.O. and Oyeyemi, E.O. Interplanetary Origins of Some Intense Geomagnetic Storms During Solar Cycle 24 and the Responses of African Equatorial/Low-Latitude Ionosphere to Them. Journal of Geophysical Research: Space Physics. 126, 2, 2021.

[11] Abdu, M.A. Equatorial spread F/plasma bubble irregularities under storm time disturbance electric fields. Journal of Atmospheric and Solar-Terrestrial Physics. 75–76, 2012.

[12] Amaechi, P.O., Oyeyemi, E.O. and Akala, A.O. Geomagnetic storm effects on the occurrences of ionospheric irregularities over the African equatorial/low-latitude region. Advances in Space Research. 61, 8, 2074–2090, 2018.
[13] Valladares, C.E., Sheehan, R., Basu, S., Kuenzler, H. and Espinoza, J. The multi-instrumented studies of equatorial thermosphere aeronomy scintillation system: Climatology of zonal drifts. Journal of Geophysical Research: Space Physics. 101, A12, 26839–26850, 1996.
[14] Ansari, K., Panda, S.K. and Jamjareegulgarn, P. Singular spectrum analysis of GPS derived ionospheric TEC variations over Nepal during the low solar activity period. Acta Astronautica. 169, 216–223, 2020.
[15] Kelley, M.C. and Heelis, R.A. The earth's ionosphere: plasma physics and electrodynamics. Academic Press, 1989.
[16] Takahashi, H., Essien, P., A. O. B. Figueiredo, C., M. Wrasse, C., Barros, D., A. Abdu, M., Otsuka, Y., Shiokawa, K., Li, G., Instituto Nacional de Pesquisas Espaciais, São José dos Campos, Brazil, Institute for Space-Earth Environmental Research, Nagoya University, Nagoya, Japan, and Institute of Geology and Geophysics, 5, 5, 1–10, 2021.
[17] Appleton, E.V. Two Anomalies in the Ionosphere. Nature. 157, 3995, 691–691. 1946.
[18] Li, M. and Parrot, M. Statistical analysis of the ionospheric ion density recorded by DEMETER in the epicenter areas of earthquakes as well as in their magnetically conjugate point areas. Advances in Space Research. 61, 3, 974–984, 2018.
[19] Sergeenko, N.P. Irregular Phenomena in Magnetically Conjugate Regions of the F2 Layer of the Ionosphere. Geomagnetism and Aeronomy. 58, 6, 823–830, 2018.
[20] Hanson, W.B. Electron temperatures in the upper atmosphere. Space Research. 5, 282–302, 1963.
[21] Bittencourt, J.A. and Sahai, Y. F-region neutral winds from ionosonde measurements of hmF2 at low latitude magnetic conjugate regions. Journal of Atmospheric and Terrestrial Physics. 40, 6, 669–676, 1978.
[22] Campbell, W. H., Matsushita, S. World maps of conjugate coordinates and L contours. Journal of Geophysical Research. 72, 3518–3521, 1967.
[23] Gulyaeva, T.L., Arikan, F., Stanislawska, I. and Poustovalova, L.V. Symmetry and asymmetry of ionospheric weather at magnetic conjugate points for two midlatitude observatories. Advances in Space Research. 52, 10, 1837–1844, 2013.
[24] Le, H., Liu, L., Yue, X. and Wan, W. The ionospheric behavior in conjugate hemispheres during the 3 October 2005 solar eclipse. Annales Geophysicae. 27, 1, 179–184, 2009.
[25] Oguti, T. Conjugate point problems. Space Science Reviews. 9, 6, 745–804, 1969.
[26] Timocin, E., Unal, I., Tulunay, Y. and Goker, U.D. The effect of geomagnetic activity changes on the ionospheric critical frequencies (foF2) at magnetic conjugate points. Advances in Space Research. 62, 4, 821–828, 2018.
[27] Unal, I. The Comparison of Responses to Geomagnetic Activity Changes of foF2 Predicted by IRI with Observations at Magnetic Conjugate Points for Middle and High Latitudes. Sakarya University Journal of Science. 619–625, 2020.
[28] Wescott, E.M. Magnetoconjugate phenomena. Space Science Reviews. 5, 507–561, 1966.
[29] Dabbakuti, J.R.K.K., Yarrakula, M., Panda, S.K., Jamjareegulgarn, P. and Haq, M.A. Total electron content prediction using singular spectrum analysis and autoregressive moving average approach. Astrophysics and Space Science. 367, 1, 8, 2022.
[30] Gordiyenko, G.I., Maltseva, O.A., Arikan, F. and Yakovets, A.F. An evaluation of the IRI-Plas-TEC for winter anomaly along the mid-latitude sector based on GIM-TEC and foF2 values. Advances in Space Research. 64, 10, 2046–2063, 2019.
[31] Shubin, V.N. and Gulyaeva, T.L. Global mapping of total electron content from GNSS observations for updating IRI-Plas model. Advances in Space Research. 69, 1, 168–175, 2022.
[32] Siddiqui, T.A., Yamazaki, Y., Stolle, C., Maute, A., Laštovička, J., Edemskiy, I.K., Mošna, Z. and Sivakandan, M. Understanding the Total Electron Content Variability Over Europe During 2009 and 2019 SSWs. Journal of Geophysical Research: Space Physics. 126, 9, 2021.
[33] Arikan, F. Regularized estimation of vertical total electron content from Global Positioning System data. Journal of Geophysical Research. 108, A12, 1469, 2003.
[34] Nayir, H., Arikan, F., Arikan, O. and Erol, C.B. Total Electron Content Estimation with Reg-Est. Journal of Geophysical Research: Space Physics. 112, A11, 2007.
[35] Sezen, U., Arikan, F., Arikan, O., Ugurlu, O. and Sadeghimorad, A. Online, automatic, near-real time estimation of GPS-TEC: IONOLAB-TEC. Space Weather. 11, 5, 297–305, 2013.
[36] Lissa, D., Srinivasu, V.K.D., Prasad, D.S.V.V.D. and Niranjan, K. Ionospheric response to the 26 August 2018 geomagnetic storm using GPS-TEC observations along 80° E and 120° E longitudes in the Asian sector. Advances in Space Research. 66, 6, 1427–1440, 2020.
[37] Mansilla, G.A. and Zossi, M.M. Ionospheric response to the 26 August 2018 geomagnetic storm along 280° E and 316° E in the South American sector. Advances in Space Research. 69, 1, 48–58, 2022.
[38] Jenan, R., Dammalage, T.L. and Panda, S.K. Ionospheric total electron content response to September-2017 geomagnetic storm and December-2019 annular solar eclipse over Sri Lankan region. Acta Astronautica. 180, 575–587, 2021.

[39] Sharma, S.K., Singh, A.K., Panda, S.K. and Ahmed, S.S. The effect of geomagnetic storms on the total electron content over the low latitude Saudi Arab region: a focus on St. Patrick's Day storm. Astrophysics and Space Science. 365, 2, 35, 2020.
[40] Pesaran, M.H., Shin, Y. and Smith, R.J. Bounds Testing Approaches to the Analysis of Level Relationships. Journal of Applied Econometrics. 16, 3, 289–326, 2001.
[41] Pesaran, M.H. and Shin, Y. An Autoregressive Distributed-Lag Modelling Approach to Cointegration Analysis. Econometrics and Economic Theory in the 20th Century. S. Strom, ed. Cambridge University Press. 371–413, 1999.
[42] Atici, R. and Sagir, S. The Effect on Sporadic-E of Quasi-Biennial Oscillation. Journal of Physical Science and Application. 6, 2, 2016.
[43] Dickey, D.A. and Fuller, W.A. Distribution of the estimators for autoregressive time series with a unit root. Journal of the American Statistical Association. 74, 366, 427–431, 1979.
[44] Phillips, P.C.B. and Perron, P. Testing for a unit root in time series regression. Biometrika. 75, 2, 335–346, 1988.
[45] MacKinnon, J.G. Numerical Distribution Functions for Unit Root and Cointegration Tests. Journal of Applied Econometrics. 11, 6, 601–618, 1996.
[46] Sağır S, Atıcı R. Jeomanyetik fırtına süresince NeQuick2 modelinin performansı. Muş Alparslan Üniversitesi Fen Bilimleri Dergisi. 2019;7(2):689–696. doi:10.18586/msufbd.650664
[47] Sagir S, Karatay S, Atici R, Yesil A, Ozcan O. The relationship between the Quasi Biennial Oscillation and Sunspot Number. Advances in Space Research. 2015;55(1):106–112. doi:https://doi.org/10.1016/j.asr.2014.09.035
[48] Atici, R. and Sagir, S. The effect of QBO on foE. Advances in Space Research. 60, 2, 357–362, 2017.
[49] Sagir, S. and Atici, R. Comparison of the QBO and F10.7 Solar Flux Effects on Total Mass Density. Geomagnetism and Aeronomy. 58, 7, 841–845, 2018.
[50] Fukushima, N. Electric potential difference between conjugate points in middle latitudes caused by asymmetric dynamo in the ionosphere. Journal of geomagnetism and geoelectricity. 31, 3, 401–409, 1979.
[51] Yamazaki Y, Maute A. Sq and EEJ—A Review on the Daily Variation of the Geomagnetic Field Caused by Ionospheric Dynamo Currents. Space Science Reviews. 2017;206(1–4):299–405. doi:10.1007/s11214-016-02